Self-consistent band structure of the rutile dioxides NbO_2, RuO_2, and IrO_2

J. H. Xu
Shanghai Institute of Metallurgy, Shanghai 200050, China

T. Jarlborg
Département de Physique de la Matière Condensée, Université de Genève, 32 boulevard d'Yuoy, CH-1211 Genève 4, Switzerland

A. J. Freeman
Department of Physics and Astronomy, Northwestern University, Evanston, Illinois 60208
(Received 5 June 1989)

The electronic structures of the rutile dioxides NbO_2, RuO_2, and IrO_2 have been determined from self-consistent semirelativistic linear muffin-tin-orbital band calculations. The basis set is completed with *s* and *p* functions from "empty spheres" inserted in the open parts of the structure. The band results are analyzed in terms of Fermi-surface features, band positions, x-ray photoemission spectra, and joint density-of-state functions. Comparisons with available experimental data are, in general, favorable. In particular, the effects from self-consistency are pointed out by comparison with earlier non-self-consistent band results.

I. INTRODUCTION

Among the oxides, the rutile-structure transition-metal dioxides exhibit a variety of interesting physical properties: RuO_2 and IrO_2 exhibit metallic conductivity at room temperature; RuO_2 especially is a corrosion-resistant low-overpotential electrode for chlorine and oxygen evolution.[1] Further, it has been reported that the catalytic photodecomposition of water into hydrogen and oxygen occurs when RuO_2 is added into a TiO_2 electrode.[2] RuO_2 is promising for use as an electrode conductor material[3] in integrated circuits,[4] because RuO_2 has excellent chemical stability and metallic conductivity. All these physical properties of RuO_2 have stimulated applied research.

On the other hand, less fundamental research work has been done, especially on the electronic structures of the rutile-structure transition-metal dioxides. The valence bands of rutile dioxides have been studied using photoemission spectroscopy.[5–8] Optical reflectivity measurements in the 0.5–0.9-eV photoenergy region were performed by Goel *et al.*[9] The Fermi surfaces of RuO_2, OsO_2, and IrO_2 have been studied by Graebner *et al.*[10] using magnetothermal oscillation measurements. The calculated electronic structure of the rutile-structure transition-metal dioxides was first reported by Mattheiss[11] using a non-self-consistent augmented-plane-wave–linear-combinations-of-atomic orbitals (APW-LCAO) method, and by Sasaki and Soga using the discrete-variational (DV)-$X\alpha$ cluster method;[12] the results were found to qualitatively agree well with each other. However, the results of Goel *et al.*[9] indicated that, as expected, Mattheiss's results overestimated the *p-d* gap by about 1 eV. For understanding a possible soft-mode phonon instability in NbO_2 a non-self-consistent LAPW calculation of NbO_2 was performed by Posternak *et al.*[13] To obtain good agreement between the calculated joint density of states and experimental ϵ_2 values, an arbitrary empirical adjustment of the *p-d* gap was suggested, and no Fermi-surface nesting feature was observed. In view of the disagreement between non-self-consistent band results[11,13] and experimental results concerning the position of the *p* and *d* bands, it was thought necessary to perform self-consistent band calculations. A further motivation is the fact that there is large charge transfer in the oxides which may not be fully accounted for in a non-self-consistent overlapping change density construction of the potential.

In this work, the electronic structures of the rutile dioxides NbO_2, RuO_2, and IrO_2 have been studied using the self-consistent semirelativistic linear muffin-tin-orbital (LMTO) method associated with the atomic sphere approximation.[14] Due to the large open space in the rutile structure, "empty spheres" have been included in the calculations.[15] Self-consistency was found to be important in positioning the oxygen 2*p* bands below the Fermi energy. In general, for RuO_2 and NbO_2, the calculated Fermi surfaces are in good agreement with either experiment[10] or an earlier calculation;[13] for IrO_2, according to Ref. 11 the spin-orbit interaction has to be taken into account in order to obtain good agreement between the calculated and the experimental results. The calculated peak positions of the XPS spectra (including matrix elements) for RuO_2 and IrO_2 are in good agreement with experiment.[5,6]

The methodology of the present calculation is described in Sec. II. Results are presented in Secs. III, IV, and V, including band structures and Fermi surfaces, x-ray photoemission spectra, and joint density of states related to optical spectra, respectively.

II. METHOD

The rutile structure has six atoms per tetragonal unit cell (cf. Fig. 1). The metal atoms occupy body-centered

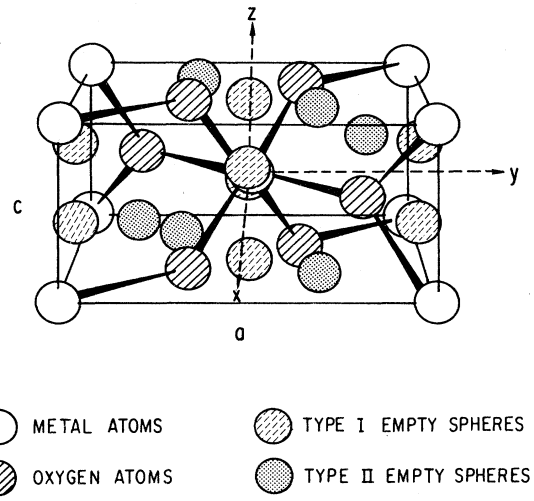

FIG. 1. The rutile-structure unit cell. The "empty" spheres used in the calculation are also indicated.

sites at (0,0,0) and $\frac{1}{2}(a,a,c)$ where a and c are the lattice parameters. For simplicity, we take $a=1$ hereafter. The oxygen atoms surround the metal site forming distorted octahedra so their positions can be written $\pm(u,u,0)$ and $(\frac{1}{2}\mp u,\frac{1}{2}\pm u,c)$ where u is about 0.31 depending on which compound is used. This makes the rutile structure rather open in which touching spheres fill only $\sim 36\%$ for RuO_2 and IrO_2 and $\sim 40\%$ for NbO_2 of the total volume. In order to make the LMTO band method suitable for studies of this (open) structure we have inserted two sets of empty spheres into the open spaces of the unit cell. The positions of these spheres are $(u,1-u,0)$, $(1-u,u,0)$, $(\frac{1}{2}\pm u,\frac{1}{2}\mp u,c/2)$ and $(0,\frac{1}{2},\pm c/4)$ (cf. Fig. 1).

Since there are two inequivalent sites for this choice of empty spheres we have totally four inequivalent potentials among the 14 sites in the unit cell. However, now the volume fraction is increased to $\sim 75\%$ and with the compact basis set including $l=2$ for the metal sites and $l=1$ for oxygen and the empty sites, the LMTO eigenvalue matrices are of the rather moderate size of 66×66. The convergence is improved by including the internal l'' summations to $l''_{\max}=3$ in the three-center terms.

We have not tested the effect of the empty spheres on the band structure, but the good band results obtained for the open structured semiconductor GaAs by use of empty spheres[15] gives us confidence that a similar technique will work well also for the MO_2 compounds which are less open than the diamond structure. Charge transfer is considerable for these oxides and it is important that the overlap Wigner-Seitz spheres ($R_{\rm WS}$) are chosen accordingly. In a test calculation for RuO_2, it was found that the discontinuity of the potentials at the sphere boundaries is small for the choice $R^{\rm Ru}_{\rm WS}=0.333a$, $R^{0}_{\rm WS}=0.291a$, $R^{E_{\rm I}}_{\rm WS}=0.172a$, and $R^{E_{\rm II}}_{\rm WS}=0.174a$. Similar (although not exact) values (since the c/a are different) were chosen also for the other compounds (cf. Table I). In addition, the calculation includes the "combined correction" terms for the overlapping spheres.[14] The core states

TABLE I. The lattice constants and radii of the overlapping Wigner-Seitz spheres for NbO_2, RuO_2, and IrO_2 where R^M is the metal WS radius, R^O that for oxygen atom, and $R^{E_{\rm I,II}}$ for the empty spheres (in a.u.).

Lattice constant (Å)	NbO_2 $a=4.841$[a] $c=2.992$	RuO_2 $a=4.4919$[b] $c=3.1066$	IrO_2 $a=4.4983$[b] $c=3.1544$
R^M	2.921	2.825	2.843
R^O	2.063	1.964	2.002
$R^{E_{\rm I}}$	1.426	1.463	1.460
$R^{E_{\rm II}}$	1.599	1.478	1.454

[a]Reference 13.
[b]Reference 11.

are treated fully relativistically and are "nonfrozen," i.e., they are relaxed in the self-consistent interactions. The valence states are treated in a semirelativistic approximation so that all relativistic terms except spin-orbit coupling are included. Other details of the self-consistent LMTO calculations can be found in Refs. 14 and 15.

The bands have been calculated at 90 k points in the irreducible ($\frac{1}{16}$) part of the Brillouin zone (cf. Fig. 2). For obtaining the bands on a finer mesh, we carried out a 43–50-parameter Fourier fitting of the bands yielding rms errors of 1–4 mRy. The band-structure plots (Fig. 3), the density-of-states (DOS) diagrams (Fig. 4), and the Fermi surfaces (FS) (Fig. 5) are all based on the Fourier representation of the bands. The maximum fitting errors reach 11–12 mRy at some symmetry points. However, for the FS structures, the maximum fitting errors are about 3 mRy. The DOS's were subsequently determined from the Fourier representation of the bands using the tetrahedron integration method[16] applied to a subdivision

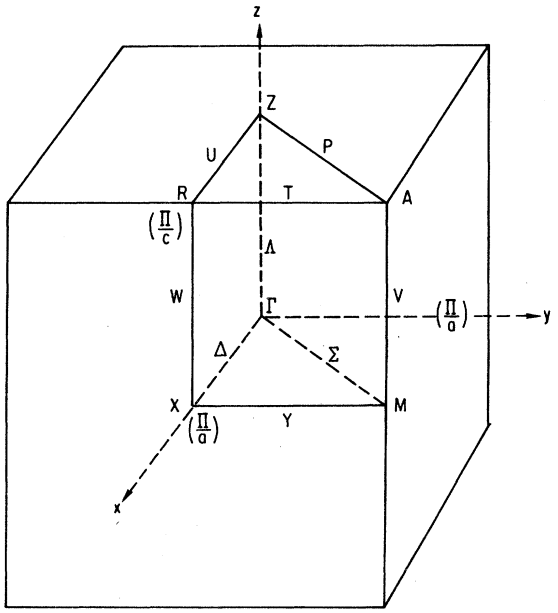

FIG. 2. The tetragonal Brillouin zone (with its irreducible part indicated).

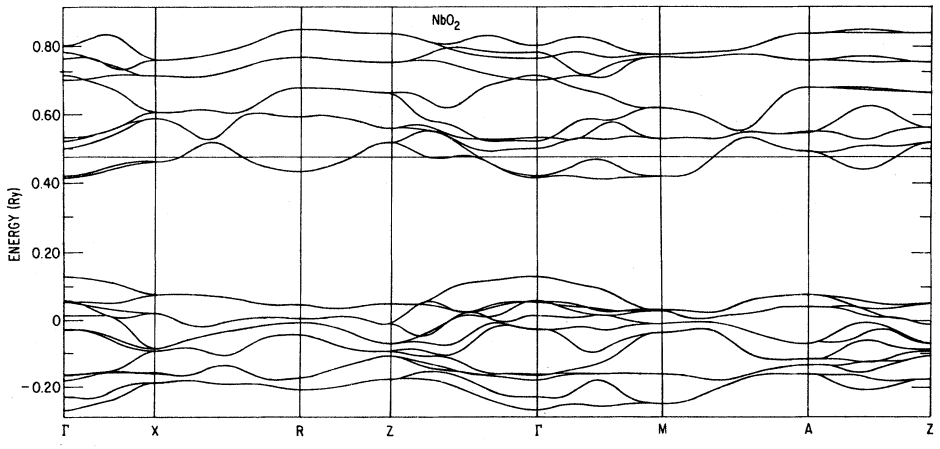

(a)

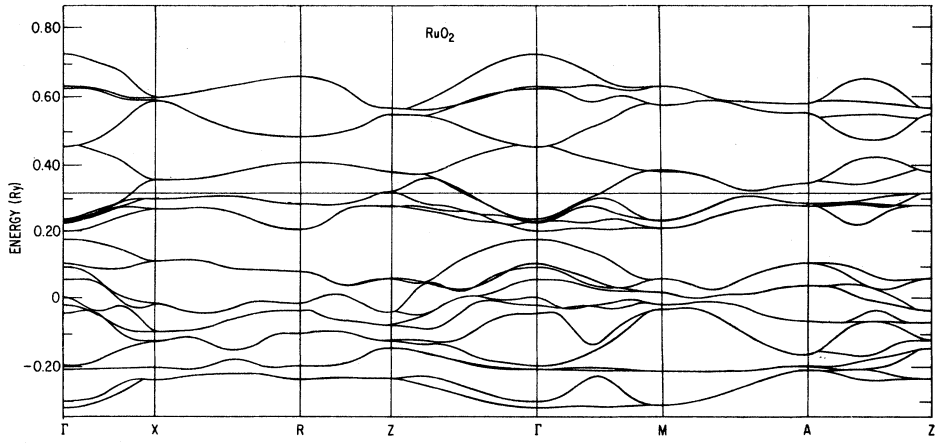

(b)

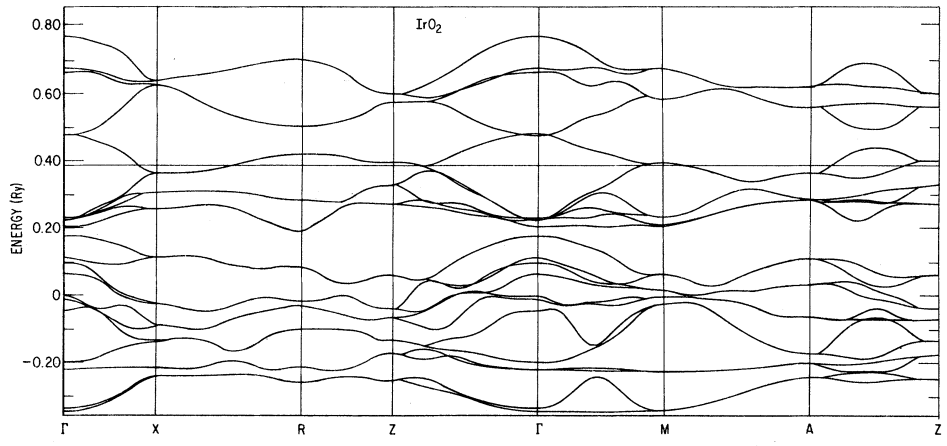

(c)

FIG. 3. The band structure along high-symmetry lines for the three compounds (a) NbO_2, (b) RuO_2, and (c) IrO_2.

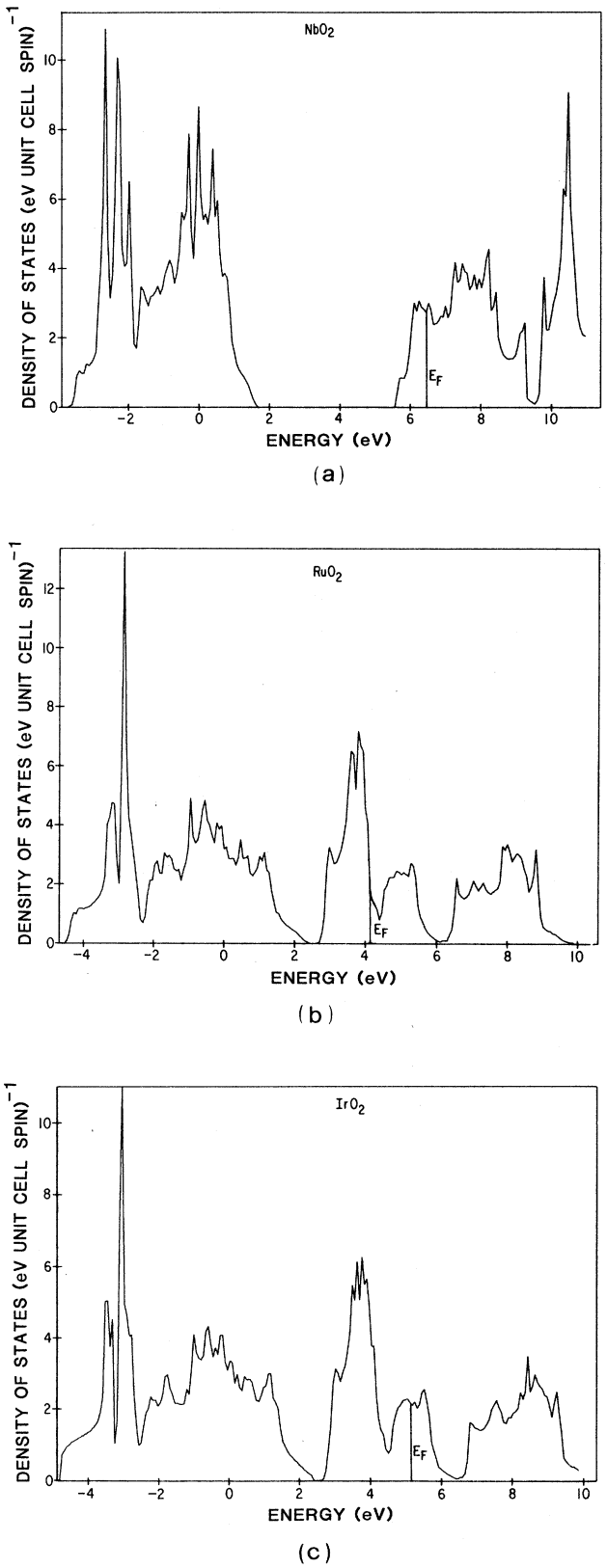

FIG. 4. Total density-of-state function for (a) NbO_2, (b) RuO_2, and (c) IrO_2. The O 2*s* states lie below the energy range shown here. The gaps shown here are between the O 2*p* and the *M d* (Nb 4*d*, Ru 4*d*, and Ir 5*d*) bands.

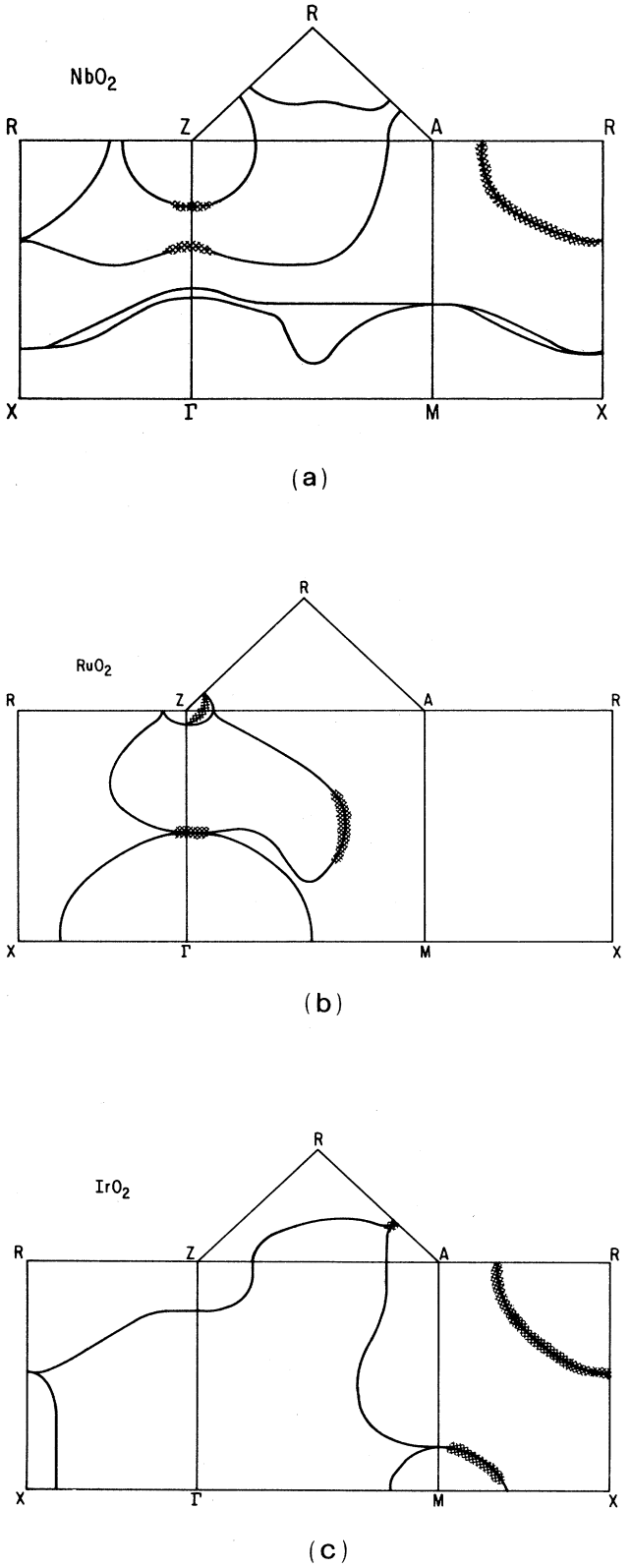

FIG. 5. The calculated Fermi surfaces for (a) NbO_2, (b) RuO_2, and (c) IrO_2. The cross hatched area denotes numerical uncertainty.

TABLE II. The conduction-band width, p-d gap, and Fermi level related to the t_{2g} bottom at Γ point for NbO_2 (in eV).

	Conduction-band width at Γ	p-d gap at Γ	E_F (related to t_{2g} bottom)
This work	5.38	4.1	0.75
Posternak *et al.*[a]	5.4	6.1	0.77

[a]Reference 13.

of the ($\frac{1}{16}$) irreducible Brillouin zone (BZ) into 3072 tetrahedrons. The DOS presented here includes a 5-mRy broadening function. The tetrahedron method is also employed for calculating the joint density of states (JDOS). For the x-ray photoemission spectra (XPS), larger broadening, ~10 mRy, is added to the final curves to include the effects of experimental broadening.

III. BAND STRUCTURES AND FERMI SURFACES

The shape of the band structures is similar in all these rutile dioxides (Fig. 3). Above the oxygen 2s band (not shown) are 12 oxygen 2p bands. The Fermi energies (E_F) fall at the lower part of the metal d bands, among the six t_{2g} subbands, while the upper four bands in the d complex have e_{2g} symmetry. The two d subbands are well separated except at the Γ point. These features are found in earlier non-self-consistent band results on the rutile structures.[11,13] However, the widths of the bands, and the gaps between them, differ sometimes considerably from the earlier calculations and are probably a result of the self-consistent treatment of the charge transfer effects included in this calculation.

Table II presents some band energies for NbO_2 and, for comparison, the previous results of Posternak *et al.*[13] As seen, there is a large difference for the p-d gap, while for the d band and the position of E_F relative to it, the agreement is good between the two calculations. Similarly, comparing our p-d gaps for RuO_2 and IrO_2 with those obtained by Mattheiss,[11] we find ours to be rather small (≤ 0.5 eV) while they are 1.5–2 eV, respectively, in the results of Mattheiss. As will be discussed later in the context of JDOS and XPS spectra, experimental results favor the smaller p-d gaps. The shapes of the Op and M d DOS functions (Fig. 4) are very similar to those from Refs. 11 and 13, except for a rigid shift (a reduction of 1.5–2 eV) of the p to d band separation. Finally, the position of the semicore O 2s band is less interesting but rather sensitive to charge transfer and therefore also to self-consistency. Experimentally (XPS),[5] the 2s peak is placed at 21.1 and 22.0 eV below E_F in RuO_2 and IrO_2, respectively. The band results put the O 2s peak at 19.6, 18.7, and 24.3 eV below E_F in NbO_2, RuO_2, and IrO_2, respectively. However, when comparing with XPS spectra for such a localized state as O 2s, one expects rather large relaxation effects from the hole left behind in the excitation process. Thus the 10–20% larger excitation energies than local density ground state band energies are not unexpected.

For the metallic d bands, one finds that a rigid band model describes the 4d and 5d materials, RuO_2 and IrO_2, quite well. The total bandwidth as well as the shape of the DOS is very similar, while the differences in band occupation place E_F differently: at 1.46 eV above the gap in RuO_2 and at 2.42 eV in IrO_2. In NbO_2, the hybridization of the Nb 4d band is different from the other two compounds because of the larger c/a ratio. Therefore one notes a different d-band structure, including a different shape of the DOS and an E_F which is only 0.75 eV above the gap.

Since the O 2p bands are completely filled and separated from the M d band through a gap, it is tempting to define the charge transfer at four electrons per M atom. However, the electron count within each WS sphere gives a quite different picture of the charge transfer (cf. Table III). This reflects the general difficulty to using the chemist's ionic model point of view of charge transfer and to compare that obtained using a WS sphere count in the LMTO approach.

The Fermi level falls at the lower part of the M d band, in the t_{2g} complex for all three compounds. The density of states of the Fermi level agrees quite well in the case of IrO_2 with that of the other calculations[11] and experiment[17] (cf. Table IV). The disagreement with the other results for RuO_2 is not understood. On the other hand, the Fermi surface is a very sensitive feature of the band structure and, as expected, the FS's are completely different for the three compounds.

Starting with NbO_2, and comparing the FS with that of Ref. 13, one sees somewhat unexpectedly that, while self-consistency made considerable changes to the band-structure—such as decreasing the Nb d to Op band

TABLE III. Charge content within the different WS spheres projected by l and atom type.

	A_s	A_p	A_d	B_s	B_p	E_s^{I}	E_p^{I}	E_s^{II}	E_p^{II}
NbO_2	0.51	0.98	2.90	1.60	4.44	0.10	0.06	0.05	0.04
RuO_2	0.60	1.06	6.17	1.60	4.17	0.12	0.09	0.05	0.04
IrO_2	0.70	1.08	6.85	1.59	4.29	0.12	0.09	0.05	0.04

TABLE IV. The density of states at E_F (per eV cell spin) with a 5-mRy broadening; for comparison the experimental data and other (non-self-consistent) calculated results are listed.

		NbO_2	RuO_2	IrO_2
Calc.	This work	2.74	2.89	2.09
	Other	2.35[a]	1.89[b]	2.02[b]
Expt.			2.44[c]	2.33[c]

[a]Reference 13.
[b]Reference 11.
[c]Reference 17.

difference—the differences in the FS are relatively small. The reason is that around E_F the states are of rather purely $4d$ character and the electron count pins E_F at a certain level independent of the energies of the completely filled bands. One band follows E_F closely along Z-Γ and gives rise to the only topological difference with the FS of Ref. 13 (but is still very uncertain due to its closeness to E_F).

We have not carried out a calculation of the generalized susceptibility $\chi(q)$ as in Ref. 13, but expect that our $\chi(q)$ will be very similar. Thus our result also supports (indirectly) the idea that the structural transformation of NbO_2 is not triggered by an anomalous behavior of $\chi(q)$ near the P point.[13] Nesting occurs for $q \sim \frac{3}{4}|\Gamma z|$ but these q values do not appear to be related to the structural transformation.

For RuO_2 and IrO_2, magnetothermal oscillation measurements have been performed and give experimental information about their Fermi surfaces.[10] The calculated FS for RuO_2 shows very good agreement with the experimental one, both regarding the topology (cf. Fig. 5) and orbit cross sections (cf. Table V). There is some improvement compared to the non-self-consistent results of Ref. 11, notably concerning the appearance of a small Z-centered ellipsoid. However, we note that using the Fourier series fitting procedure there is an uncertainty concerning possible band crossings: In RuO_2 a band crossing appears as a small gap on the MA line, which in-

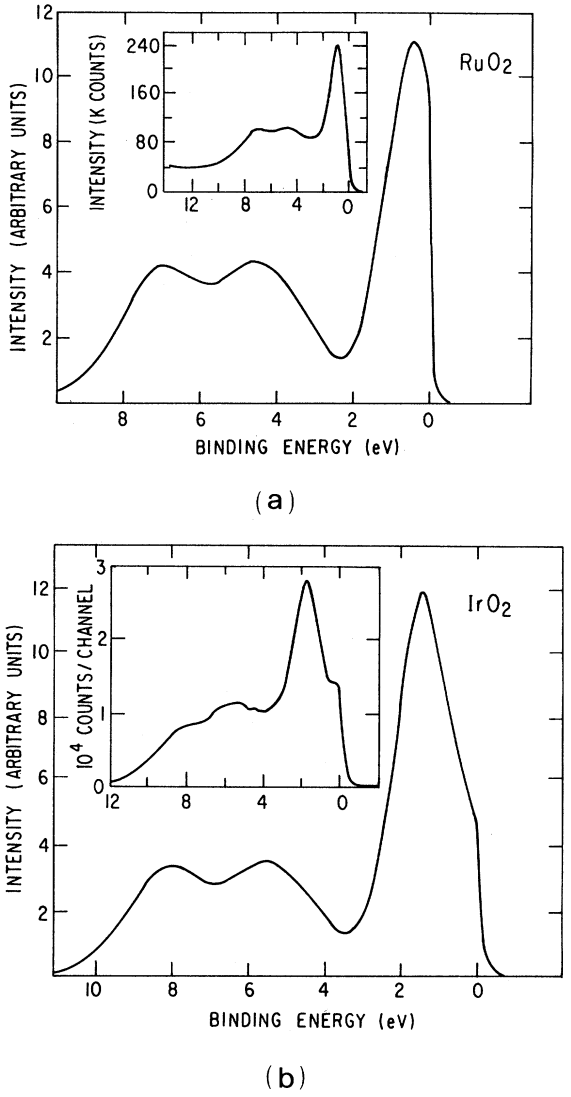

FIG. 6. Comparison of the calculated XPS spectra of (a) RuO_2, and (b) IrO_2 with the experimental observations of (a) Ref. 5 and (b) Ref. 6.

TABLE V. Comparison of calculated radii with experiment for the Fermi-surface cross sections at high-symmetry directions for RuO_2 and IrO_2 (in Å^{-1}).

				Z-centered ellipsoid			
		$\epsilon_{\Gamma M}, \epsilon_{\Gamma X}$	$\epsilon_{\Gamma Z}$	ZR	$Z\Gamma$		
RuO_2	Expt.[a]	0.520	0.445	0.155	0.095		
	Calc.	0.52	0.46	0.10	0.06		
		ϵ_{ZA}	$\epsilon_{\Gamma Z}$	θ_{AR}	θ_{AZ}	$\lambda_{M\Gamma}$	λ_{MX}
IrO_2	Expt.[a]	0.19	0.228	0.21	0.17	0.232	0.335
	Calc.	0.22	0.22	0.21	0.23–0.26	0.19	0.26–0.27
		λ_{MA}	ρ_{RA}	ρ_{RX}			
	Expt.[a]	0.288	0.31	0.235			
	Calc.	0.19	0.44–0.47	0.48			

[a]Reference 10.

TABLE VI. Comparison of the peak positions of the calculated and the experimental XPS data of the rutile doixides NbO_2, RuO_2, and IrO_2 (in eV).

		1	2	3
NbO_2	Calc.	0.0	6.5	8.7
RuO_2	Calc.	0.54	4.6	7.0
	Expt.[a]	0.6	4.7	6.9
	b	1.2	3.8, 5.8	7.35
IrO_2	Calc.	1.5	5.6	8.1
	Expt.[c]	1.7	5.7	7.9
	b	1.5	5.6, 7.75	10.6

[a]Reference 5.
[b]Reference 8.
[c]Reference 6.

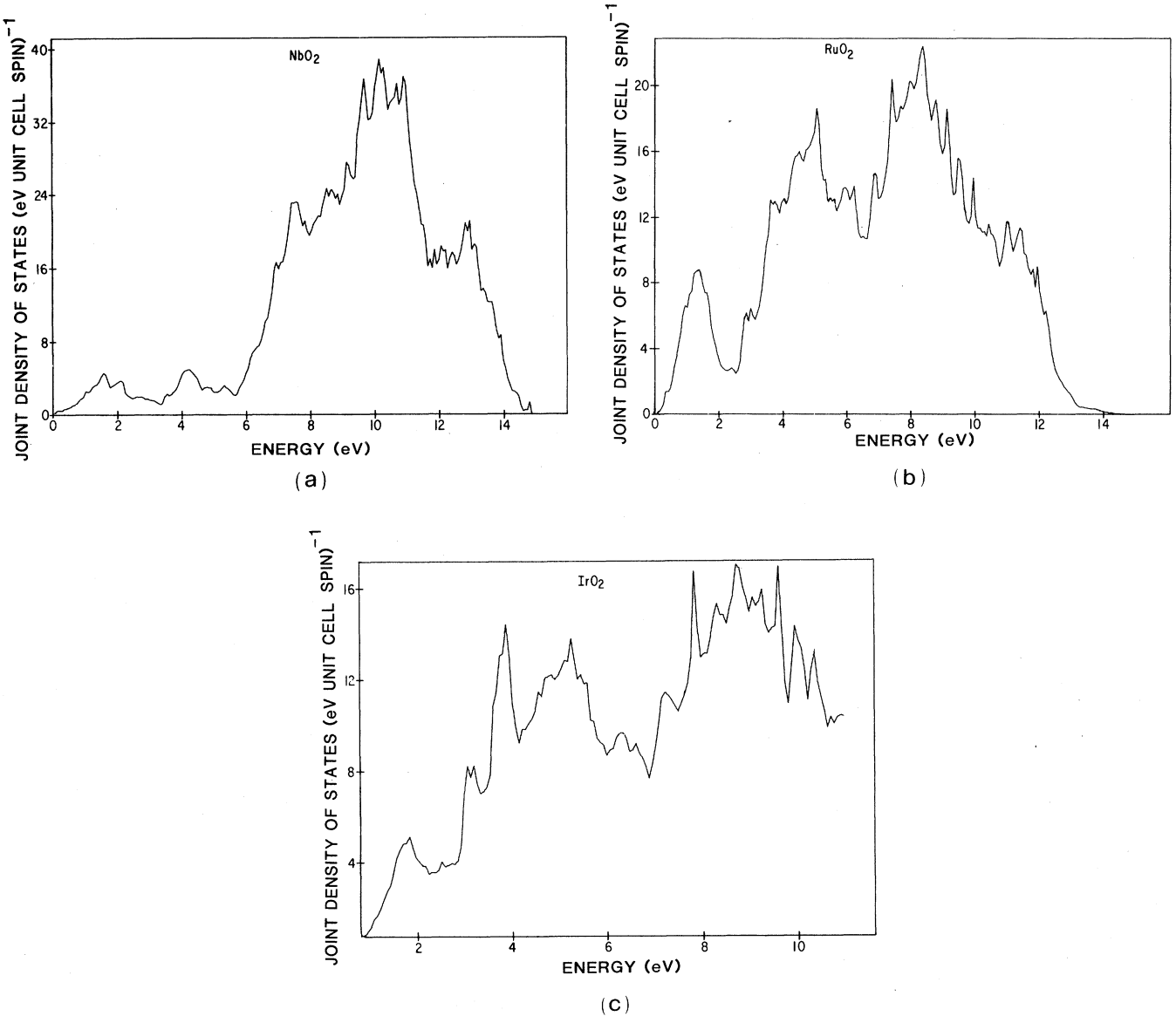

FIG. 7. Joint DOS for (a) NbO_2, (b) RuO_2, and (c) IrO_2.

troduces an uncertainty about the Fermi surface in this region. For IrO_2 a small improvement is seen, in our self-consistent results; the state at M is raised in energy slightly to form a hole pocket around M with almost the same dimensions as found experimentally. At other regions of the BZ there are some obvious disagreements with the experimental FS. However, as was shown in Ref. 11, the inclusion of a $5d$ spin-orbit coupling (amounting to 33 mRy) will essentially strike out these disagreements and split the degenerate orbits indicated by λ in Table V and in Ref. 10.

IV. X-RAY PHOTOEMISSION SPECTRA

From XPS measurements one can usually determine valence-band energies down to a resolution of $\frac{1}{2}$ eV or finer. These data are normally taken on polycrystalline samples and one is restricted to compare with peak positions in the calculated DOS rather than the band structure. Some of this analysis was presented earlier in the discussion of the band results. Here we want to include matrix-element effects, which reshape the XPS spectra from that of the superimposed partial DOS, and give, indirectly, information about the character of the band states. Our calculations follow the method of Ref. 18, valid for polycrystalline averaging of directional variations. The final state is assumed to be in a high-level free-electron continuum and the dipole matrix element with the initial band state is calculated using the "acceleration" form, i.e., where the radial derivative of the potential is the operator. Due to the high density of states, no **k**-conservation rule is applied. No relaxation effects are included but as long as the initial state is a delocalized valence state and the final state is highly excited free-electron-like, one can assume relaxation effects to be small. The calculated XPS spectra are broadened with a Gaussian function to account for experimental broadening effects. The broadening is sometimes rather striking in its consequences in that small adjacent peaks can be merged into one larger peak.

In Table VI we show calculated peak positions, together with available experimental data,[5,6,8] for band features associated with O p and M d levels. In Fig. 6 we show the calculated XPS spectra for RuO_2 and IrO_2 together with the measured curves.[5,6] The agreement is good concerning both the peak positions and the shape of the curves. (No XPS measurements on NbO_2 are known to us.) The most notable effect of the matrix elements is the comparatively large M d XPS cross section over that of O p, making the XPS curves rather different from the total DOS curves (cf. Fig. 4).

More recently, the electronic structures RuO_2 and IrO_2 were studied by soft x-ray photoemission spectroscopy with synchrotron radiation.[8] As shown in Table VI, the calculated peak positions of RuO_2 are found to be in reasonable agreement with these experiments with the largest discrepancy being in the lowest-energy peak. By contrast, there is good agreement in the case of IrO_2 except for the highest-energy peak; in that case the disagreement between the two experimental results is so large that reexamination of the data is called for.

Similar matrix-element calculations can be applied also for core states. However, as mentioned earlier, the peak positions for XPS-excited core levels are strongly affected by relaxation of the remaining localization hole state. Thus the core levels appear more strongly bound that found from the calculated core-level energies. This is also the case for the semi-core levels like the oxygen $2s$ state.

V. JOINT DOS AND RELATION TO OPTICAL SPECTRA

The calculation of ultraviolet photoemission spectra (UPS) and optical spectra, which is related to the imaginary part of the dielectric function $\epsilon_2(\omega)$, is difficult, mainly due to large relaxation effects of the final state. In principle, one knows from the band results both the initial- and final-state wave functions, and now obeying the **k**-conservation rule, a calculation of the spectra is possible. But the calculated band structure above E_F is for zero occupation of these states. When an electron occupies one of these states, the relaxation process is complicated and difficult to include in a calculation. Here we have restricted our study to a calculation of the joint DOS, i.e., obeying **k** conservation, using constant matrix elements and no relaxation of the band structure. Further, we assume that no excited states other than those included in our band-structure basis are of importance.

In Fig. 7 we show the JDOS curves up to 10–14 eV, obtained for the three compounds. For NbO_2 the JDOS is rather low up to 6 eV due to the relatively large Nb d to O p band separation. Recent optical measurements[9] up to 9.5 eV show peaks in the ϵ_2 curves at 2.5–3, ~4.9, and ~7.5 eV for RuO_2 and at 1.5–2 eV and several peaks in the interval 3.7–7.7 eV for IrO_2. (These measurements were performed for two different surface orientations and hence give some differences on a fine energy scale.) Our JDOS curves have, in addition to finer details, broad double peak structures at ~5 and ~8.5 eV (RuO_2) and at 4–5 and ~9 (IrO_2). For RuO_2, the finer peaks at 2.9, 4.9, and 7.4 eV may correspond to the measured structures; the peaks at ~3.8 eV coincide with a weak shoulder measured at one orientation near 4 eV. Tracking the peaks by means of their relative heights is more risky due to the neglect of matrix elements. Similarly, for IrO_2 five peaks in the JDOS at 3.2, 3.9, 5.2, 6.2, and 7.8 eV (with the middle one being the strongest) can be compared with five measured peaks in the interval 4–7.6 eV for one orientation. A strong peak measured near 1.2 eV is considerably lower than the possible peak in the JDOS at ~1.8–2.0 eV. Thus in these crude comparisons between experiment and calculation one has to admit relaxation effects of the order of 0.5–1 eV, which also might be state dependent. An analysis of the orientational dependence of the JDOS has not been done here.

ACKNOWLEDGMENTS

This work was supported by a grant from the Air Force Office of Scientific Research (Grant No. 81-0024). We are grateful to F. Pollak for stimulating this research and for helpful discussions.

[1]A. T. Kuhn and C. J. Mortimer, J. Electrochem. **120**, 231 (1973); S. Puschaver, Chem. Ind. (London) **236**, 52 (1975); A. Trasatti and G. Buzzance, J. Electroanal. Chem. Interfacial Electrochem. **29**, 635 (1971); L. D. Burke, O. J. Murphy, J. F. O'Neill, and S. Venkatesan, J. Chem. Soc. Faraday Trans. I **73**, 1659 (1977).

[2]T. Kawai and T. Sakata, Chem. Phys. Lett. **72**, 87 (1980).

[3]S. Staki and R. Muller (unpublished).

[4]D. J. Pedder, Electrocomp. Sci. Tech. **2**, 259 (1976); M. W. Shafer and J. Armstrong, IBM Tech. Discl. Bull. **20**, 4633 (1978).

[5]J. Riga, C. Tenret-Noël, J. J. Caudano, J. J. Verbist, and Y. Gobillon, Phys. Scr. **16**, 351 (1977).

[6]G. K. Wertheim and H. J. Guggenheim, Phys. Rev. B **22**, 4680 (1980).

[7]N. Beatham and A. F. Orchard, J. Electron Spectrosc. Relat. Phenom. **16**, 77 (1979).

[8]R. R. Daniel, G. Margaritondo, C. A. Georg, and F. Levy, Phys. Rev. B **29**, 1813 (1984).

[9]A. K. Goel, G. Skorinko, and F. H. Pollak, Solid State Commun. **39**, 245 (1981); A. K. Skorinko and F. H. Pollak, Phys. Rev. B **24**, 7342 (1981).

[10]J. E. Graebner, E. S. Greiner, and W. E. Ryden, Phys. Rev. B **13**, 2426 (1976).

[11]L. F. Mattheiss, Phys. Rev. B **13**, 2433 (1976).

[12]T. A. Sasaki and T. Soga, Physica B+C **111B**, 304 (1981).

[13]M. Posternak, A. J. Freeman, and D. E. Ellis, Phys. Rev. B **19**, 6555 (1979).

[14]O. Anderson, Phys. Rev. B **12**, 3060 (1975); T. Jarlborg and G. Arbman, J. Phys. F **6**, 189 (1976).

[15]T. Jarlborg and A. J. Freeman, Phys. Lett. **74A**, 349 (1979).

[16]J. Rath and A. J. Freeman, Phys. Rev. B **11**, 2109 (1979).

[17]B. C. Passenheim and D. C. McCollum, J. Chem. Phys. **51**, 320 (1969).

[18]T. Jarlborg and P. O. Nilsson, J. Phys. C **12**, 265 (1979).